RSC Advances

PAPER

View Article Online
View Journal | View Issue



Cite this: *RSC Adv.*, 2022, **12**, 8474

# An *in situ* DRIFTS study on nitrogen electrochemical reduction over an Fe/$BaZr_{0.8}Y_{0.2}O_{3-\delta}$-Ru catalyst at 220 °C in an electrolysis cell using a $CsH_2PO_4/SiP_2O_7$ electrolyte

Yao Yuan,[a] Naoya Fujiwara,[a] Shohei Tada [b] and Ryuji Kikuchi *[a]

Received 12th January 2022
Accepted 11th March 2022

DOI: 10.1039/d2ra00224h

rsc.li/rsc-advances

*In situ* DRIFTS measurements of an Fe/BZY-Ru cathode catalyst in an electrolysis cell using a $CsH_2PO_4/SiP_2O_7$ electrolyte were carried out in a mixed $N_2$–$H_2$ gas flow under polarization. The formation of $N_2H_x$ species was confirmed under polarization, and an associative mechanism in the electrochemical NRR process was verified.



$NH_3$ production contributes about 2% of the world's energy consumption annually, and most of the consumption is from the strongly endothermic steam reforming of methane (SRM) at 800–1000 °C in the Haber–Bosch process. Other major energy consuming processes include $CO_2$ removal, reactant gas purification, reactant gas compression for $NH_3$ synthesis, and $NH_3$ separation.[1] Due to its high energy density, $NH_3$ was expected to be a promising energy carrier in recent years.[2] $NH_3$ produced by renewable energy sources can be used as a carbon-free energy carrier. One of the promising methods to utilize renewable energy sources for $NH_3$ production is electrochemical $N_2$ reduction. Various electrolysis cells with solid and liquid electrolytes have been reported for electrochemical $N_2$ reduction over a wide temperature range. For the electrochemical $N_2$ reduction reaction (NRR) at low temperatures ($T$ < 100 °C), the main limitation is the difficulty of $N_2$ activation and the low solubility of $N_2$ in aqueous media. High temperatures ($T$ > 500 °C) can lead to decomposition of the produced $NH_3$. Hence, an electrochemical NRR at intermediate temperatures is desirable. Phosphates such as $CsH_2PO_4$ and $CsH_5(PO_4)_2$ are typically used as electrolytes at intermediate temperatures. These inorganic oxyacid salts have high proton conductivity and stability. $CsH_2PO_4$ mixed with $SiP_2O_7$ as a matrix exhibits a proton conductivity of *ca.* $1 \times 10^{-2}$ S cm$^{-1}$ at 220 °C.[3] In our previous work on electrochemical $NH_3$ synthesis using an Fe/BZY-$RuO_2$ catalyst and $CsH_2PO_4/SiP_2O_7$ electrolyte at 220 °C and ambient pressure, the highest current efficiency of 7.1% and the highest $NH_3$ yield rate of $4.5 \times 10^{-10}$ mol (s$^{-1}$ cm$^2$) were achieved at −0.4 V (*vs.* open circuit voltage (OCV)) and −1.5 V, respectively. In addition, $N_2H_4$ was successfully detected at −0.2 V (*vs.* OCV), which indicated an associative mechanism,[4] which is one of the two main reaction mechanisms in $NH_3$ synthesis, namely, associative and dissociative mechanisms. In the associative mechanism the N≡N bond in a $N_2$ molecule adsorbed on the catalyst surface is cleaved after an H atom attaches to the N atom of the adsorbed $N_2$ molecule, whereas in the dissociative mechanism the N≡N bond is broken on the catalyst surface before an H atom attaches to the $N_2$ molecule.

Typical electrochemical characterizations such as impedance spectroscopy,[5,6] current–voltage curve (*IV* curve) testing,[7,8] cyclic voltammetry,[9] and potentiostatic pulse experiment[10] can only provide indirect information on surface reactions at the electrode. It is indispensable to analyse directly adsorbed species on the electrode catalysts for the understanding of the reaction mechanism. *In situ* spectroscopy is making rapid progress and has already been applied to electrochemical devices, providing valuable information of the chemical species during the reactions.[11] *In situ* diffuse reflectance infrared Fourier transform spectroscopy (DRIFTS) for electrolysis cells attracts much attention recently.[12,13] *In situ* DRIFTS has recently become a powerful tool for investigating the reaction pathway in electrochemical $N_2$ reduction reaction.[14–16] In DRIFTS, infrared (IR) beam irradiates the sample disk, and then can be reflected at or transmitted through the sample disk. The scattered IR beam is collected by the spherical focusing mirrors and finally converted by a detector.

In this work, a commercial DRIFTS setup was modified and applied to electrochemical $N_2$ reduction as shown in Fig. 1. To enable an operation temperature higher than 200 °C that is requisite for proton conduction in the electrolyte, an electrical heating wire was placed in the base near the micro-cup. The temperature was measured by a thermocouple located next to the heating wire. An electrolysis cell was set on the micro-cup of the metal base. For protection of the ZnSe window from oxidation at the high operating temperature, a water-cooling

[a]*Department of Chemical System Engineering, The University of Tokyo, 7-3-1, Hongo, Bunkyo-ku, Tokyo 113-8656, Japan. E-mail: rkikuchi@chemsys.t.u-tokyo.ac.jp*
[b]*Department of Materials Sciences and Engineering, Ibaraki University, Ibaraki, 316-8511, Japan*

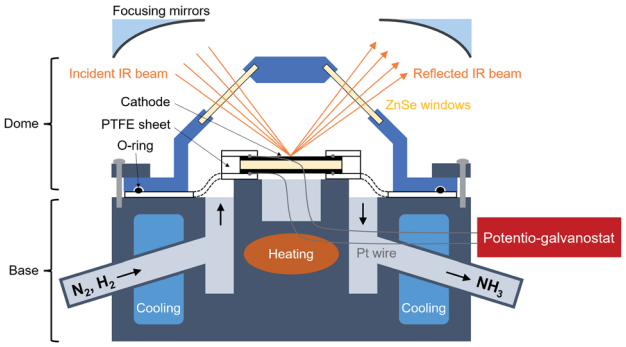


Fig. 1 A schematic of modified DRIFTS setup applied to electrochemical $N_2$ reduction. The temperature of the electrolysis cell is measured at the same place where it is heated.

system was attached to the metal base near the dome to keep the temperature of the window below 200 °C. The specific size of the apparatus is shown in the Fig. 2. An O-ring fits to the dome can ensure gas tightness of the small space in the dome. There are three pathways which connect the inside space of the dome and atmosphere. Two of them are used for the inlet and outlet gas flows, and the one connecting directly with the micro-cup was used for Pt lead wires. To avoid a short-circuit between the two Pt lead wires, a thin polyimide film (12.5 μm thick, Kapton, Dupont, Delaware, United States) which is stable from −269 to +400 °C was used to cover the Pt wires.

In our previous study of the electrochemical $NH_3$ synthesis process at 220 °C, a ø 10 mm carbon paper was used on the cathode side to increase the current collection area.[4] However, in the *in situ* DRIFTS tests, the cathode catalysts must be exposed to the IR beam, hence a carbon ring with an inside diameter of 7 mm was used instead as shown in Fig. 3. On the anode side, a ø 10 mm Pt/C loaded on carbon paper was used for current collection. The electrolysis cell consists of 0.1 g $SiP_2O_7$/$CsH_2PO_4$ electrolyte (mix ratio of $SiP_2O_7$ : $CsH_2PO_4$ was 1 : 1) compressed with 0.035 g Fe/BZY-Ru (mix ratio of Fe/BZY : $RuO_2$ was 1 : 1) catalyst on the top layer. In our previous work of the electrochemical $NH_3$ synthesis using Fe/BZY-$RuO_2$, we have successfully detected $N_2H_4$ as well as $NH_3$, which indicated the triple bond of $N_2$ was broken simultaneously with the addition of H. Fe/BZY was prepared in the same way

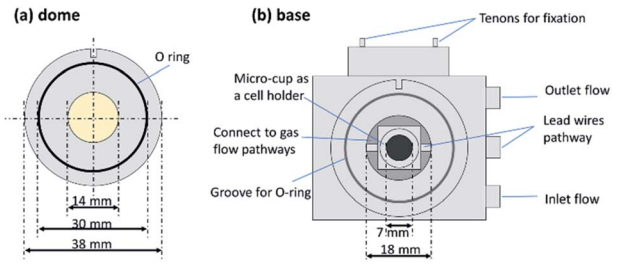


Fig. 2 (a) The bottom-up view of the dome. (b) The vertical view of the metal base.

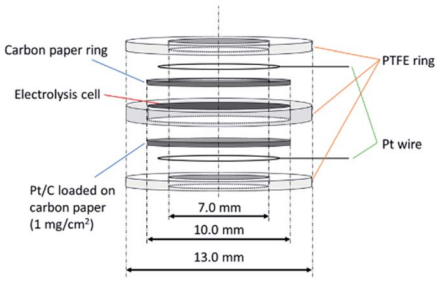


Fig. 3 A schematic of electrolysis cell on the micro-cup.

as in the previous work.[4] The as-prepared Fe/BZY powder was mixed with $RuO_2$ powder, and then the mixture was reduced in $H_2$ flow at 220 °C for 1 h. To fix the electrolysis cell, the current collection materials and the Pt lead wires, PTFE sheets (Gore Hyper-Sheet Gasket, W. L. Gore & Associate, Inc., Delaware, USA) formed into rings were used as the support. The experimental conditions in the dome are similar to those in a single-chamber reactor. The inlet gas is a mixture of $N_2$ and $H_2$, which is different from the two-chamber reactor in electrolysis tests in the previous work. A background spectrum was measured under $H_2$ gas flow of 8 mL $min^{-1}$ at 160 °C with 100 scans at OCV. All DRIFTS spectra are displayed as $\log(I_0/I)$ where $I_0/I$ is the relative reflectance ($I_0$ is the background reflectance). Then the measurements were carried out under $N_2$ gas flow of 8 mL $min^{-1}$ at 300 °C at OCV and under mixed $N_2$ and $H_2$ gas flow (both are 8 mL $min^{-1}$) at 250 °C at OCV and various applied biases.

According to the results in Fig. 4, three kinds of sharp peaks at 1050, 1300 and 1540 $cm^{-1}$, and a broad peak at 3300 $cm^{-1}$ were observed. Peak at 1050 $cm^{-1}$ is attributed to N–N stretching (reported at 1106 $cm^{-1}$),[17] which appeared in all experimental conditions even when only $N_2$ gas was supplied.

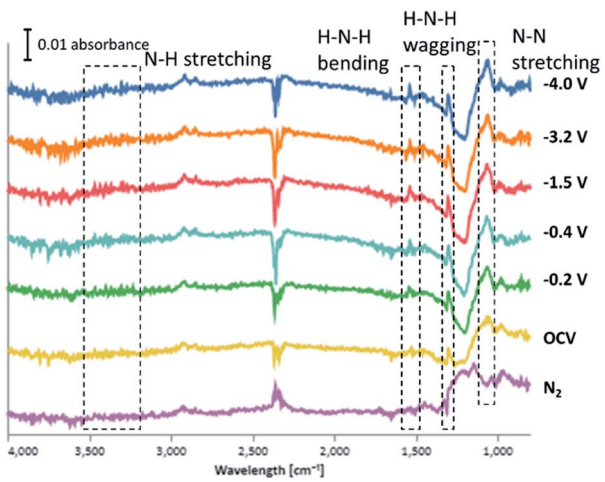


Fig. 4 Electrochemical *in situ*-FTIR spectra of the NRR on the Fe/BZY-Ru electrode at various electrochemical potentials. Then the measurements were carried out under $N_2$ at 300 °C at OCV and under mixed $N_2$ and $H_2$ at 250 °C at OCV, −0.2, −0.4, −1.5, −3.2 and −4.0 V.

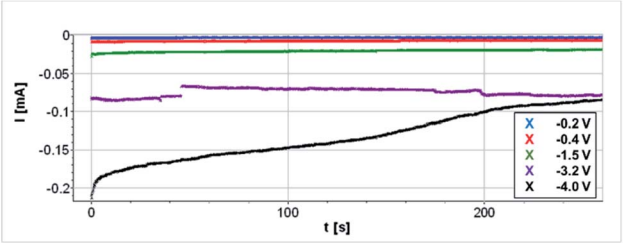


Fig. 5 Currents for applied voltages of −0.2 V, −0.4 V, −1.5 V, −3.2 V, and −4.0 V.

This implies that the $N_2$ adsorption sites on the catalyst surface are highly active. Peaks at 1300, 1540 and 3300 $cm^{-1}$ are assigned to H–N–H wagging, H–N–H bending and N–H stretching (reported at 1270, 1461 and 3235 $cm^{-1}$).[17] These three kinds of peaks appeared only when both $N_2$ and $H_2$ were supplied, and seem to become stronger with applied bias. It is obvious that $N_2H_x$ species, which can be intermediate species in the associative mechanism, were formed on the surface of Fe/BZY-Ru. The peak at 900 $cm^{-1}$ is probably attributed to $NH_3$ gas.[18] It is likely that the peaks at 1400 $cm^{-1}$ and 2800 $cm^{-1}$ are assigned to $NH_4^+$.[19] The strong signal at 2360 $cm^{-1}$ is associative with gas-phase $CO_2$ that exists in IR beam path outside the dome.

Only quite low current densities were able to be loaded as shown in Fig. 5. Reactant gases were introduced to the system without humidification, which might have led to low proton conductivity and electrolyte decomposition. In addition, current collection area of the carbon paper ring on the cathode side is small.

*In situ* DRIFTS measurements were carried out in a $N_2$–$H_2$ gas mixture under polarization, which corresponds to a situation in a single-chamber reactor. The background was measured in $H_2$ flow, and the sample measurements were carried out in a mixed $N_2$–$H_2$ gas flow. In the obtained spectra, a peak at 1100 $cm^{-1}$ was assigned to N–N stretching, and those at 1301, 1600, and 3300 $cm^{-1}$ were assigned to –$NH_2$ wagging, H–N–H bending, and N–H stretching. The intensity of the H–N–H wagging peak was enhanced by increasing the applied voltage. Appearance of these peaks confirmed the formation of $N_2H_x$ ($1 \leq x \leq 4$) species in the NRR process and consequently demonstrated that NRR proceeded *via* an associative mechanism over Fe/BZY-Ru cathode catalyst on a $SiP_2O_7$/$CsH_2PO_4$ electrolyte.

## Author contributions

Yao Yuan: investigation, data curation, formal analysis, writing – original draft. Naoya Fujiwara: methodology, resources, visualization. Shohei Tada: methodology, data curation, formal analysis. Ryuji Kikuchi: conceptualization, supervision, writing – review & editing.

## Conflicts of interest

There are no conflicts to declare.

## Acknowledgements

A part of this work was supported by Japan Society for the Promotion of Science (JSPS) KAKENHI Grant Number JP20J14232, Japan, and Japan Science and Technology Agency (JST) Core Research for Evolutional Science and Technology (CREST) Grant Number JPMJCR1441, Japan.

## References

1 I. Rafiqul, C. Weber, B. Lehmann and A. Voss, *Energy*, 2005, **30**, 2487–2504.
2 N. V. Rees and R. G. Compton, *Energy Environ. Sci.*, 2011, **4**, 1255–1260.
3 N. Fujiwara, H. Nagase, S. Tada and R. Kikuchi, *ChemSusChem*, 2021, **14**, 417–427.
4 Y. Yuan, S. Tada and R. Kikuchi, *Mater. Adv.*, 2021, **2**, 793–803.
5 R. Lan and S. Tao, *RSC Adv.*, 2013, **3**, 18016–18021.
6 B. Xu, L. Xia, F. Zhou, R. Zhao, H. Chen, T. Wang, Q. Zhou, Q. Liu, G. Cui, X. Xiong, F. Gong and X. Sun, *ACS Sustainable Chem. Eng.*, 2019, **7**, 2889–2893.
7 P. Shen, Y. Liu, Q. Li and K. Chu, *Chem. Commun.*, 2020, **56**, 10505–10508.
8 Q. Fan, C. Choi, C. Yan, Y. Liu, J. Qiu, S. Hong, Y. Jung and Z. Sun, *Chem. Commun.*, 2019, **55**, 4246–4249.
9 K. Fricke, F. Harnisch and U. Schröder, *Energy Environ. Sci.*, 2008, **1**, 144–147.
10 Y. Jännsch, J. J. Leung, M. Hämmerle, E. Magori, K. Wiesner-Fleischer, E. Simon, M. Fleischer and R. Moos, *Electrochem. Commun.*, 2020, **121**, 106861.
11 M. F. Baruch, J. E. Pander, J. L. White and A. B. Bocarsly, *ACS Catal.*, 2015, **5**, 3148–3156.
12 D. J. Cumming, C. Tumilson, S. F. R. Taylor, S. Chansai, A. V. Call, J. Jacquemin, C. Hardacre and R. H. Elder, *Faraday Discuss.*, 2015, **182**, 97–111.
13 N. Shi, Y. Xie, D. Huan, Y. Yang, S. Xue, Z. Qi, Y. Pan, R. Peng, C. Xia and Y. Lu, *J. Mater. Chem. A*, 2019, **7**, 4855–4864.
14 Y. Yao, S. Zhu, H. Wang, H. Li and M. Shao, *J. Am. Chem. Soc.*, 2018, **140**, 1496–1501.
15 X. Qu, L. Shen, Y. Mao, J. Lin, Y. Li, G. Li, Y. Zhang, Y. Jiang and S. Sun, *ACS Appl. Mater. Interfaces*, 2019, **11**, 31869–31877.
16 J.-T. Ren, C.-Y. Wan, T.-Y. Pei, X.-W. Lv and Z.-Y. Yuan, *Appl. Catal., B*, 2020, **266**, 118633.
17 P. Song, H. Wang, L. Kang, B. Ran, H. Song and R. Wang, *Chem. Commun.*, 2019, **55**, 687–690.
18 S. Süzer and L. Andrews, *J. Chem. Phys.*, 1987, **87**, 5131–5140.
19 C. Sun and D. Xue, *CrystEngComm*, 2015, **17**, 2728–2736.